Article

Effect of Carbon Content in Wheat Straw Biochar on N$_2$O and CO$_2$ Emissions and Pakchoi Productivity Under Different Soil Moisture Conditions

Amar Ali Adam Hamad [1,†], Lixiao Ni [1], Hiba Shaghaleh [1,†] , Elsayed Elsadek [2,3] and Yousef Alhaj Hamoud [2,*]

[1] College of Environment, Hohai University, Nanjing 210098, China
[2] College of Hydrology and Water Resources, Hohai University, Nanjing 210098, China
[3] Agricultural and Biosystems Engineering Department, College of Agriculture, Damietta University, Damietta 34517, Egypt
* Correspondence: yousef-hamoud11@hhu.edu.cn
† These authors contributed equally to this work.

Abstract: Agricultural soils are a primary source of greenhouse gas (GHG) emissions. Biochar is commonly used as a soil amendment to prevent climate change by reducing GHG production, increasing soil carbon storage, improving soil moisture retention, and enhancing crop productivity. However, the impact of biochar's carbon content under subsurface drip irrigation (SDI) has not been well studied. Here, we investigated the effect of different carbon (C) contents in wheat biochar under different SDI depths on soil nitrous oxide (N$_2$O), carbon dioxide (CO$_2$), soil moisture distribution, and Pakchoi productivity. A pot experiment was conducted using three SDI depths, emitters buried at 0.05, 0.10, and 0.15 m below the soil's surface, and three levels of C content named zero biochar (CK), 50% C (low (L)), and 95% C (high (H)) in greenhouse cultivation. The findings showed biochar significantly decreased N$_2$O and CO$_2$ emissions. Compared to CK, the L and H treatments decreased N$_2$O by (18.20, 28.14%), (16.65, 17.51%), and 11.05, 18.65%) under SDI$_5$, SDI$_{10}$, and SDI$_{15}$, respectively. Similarly, the L and H treatments decreased CO$_2$ by (8.05, 31.46%), (6.96, 28.88%), and (2.97, 7.89%) under SDI$_5$, SDI$_{10}$, and SDI$_{15}$, respectively. Compared to CK, L and H increased soil moisture content. All plant growth parameters and yield traits were enhanced under SDI$_5$. In summary, biochar addition significantly decreased soil N$_2$O and CO$_2$ emissions compared to CK, and increased growth performance and yield, and maintained soil moisture content. The H treatment significantly reduced N$_2$O and CO$_2$ emissions, increased plant growth and yield, and maintained soil moisture content compared to the L treatment. Soil moisture was reduced vertically and horizontally with increased radial distance from the emitter.

Keywords: N$_2$O and CO$_2$ emissions; pakchoi cabbage; subsurface drip irrigation; irrigation depths

1. Introduction

Climate change is a serious environmental problem due to the increasing population and expansion of agricultural lands. N$_2$O and CO$_2$, the leading greenhouse gases (GHGs), are emitted constantly into the atmosphere. By reducing emissions and increasing GHG sequestration, the production of biochar, and its application to the soil, will positively impact soil fertility and increase crop production [1]. Numerous studies have shown biochar is a practical approach with potential advantages for the environment and agriculture [2]. In general, biochar promotes soil carbon sequestration [3], reduces the emissions of ammonia and CO$_2$ [4], lowers soil compactness, optimizes compost [5], increases nutrients for plants, enhances water retention, and increases soil pH [6]. Previous research has assessed the adverse impacts of biochar application on soil physical and chemical properties such as soil pH, porosity, bulk density, and organic matter (OM) [7–9].

Strategies such as subsurface drip irrigation (SDI) and deficit irrigation aim to improve water-use efficiency (WUE), while ensuring adequate irrigation, by reducing water usage. These strategies attempt to decrease water loss and preserve water resources available for agricultural production [10,11]. Alternate drying and wetting techniques have been demonstrated to decrease water usage by up to 33% under rice cultivation [12]. In addition to water recycling and the adoption of localized irrigation systems such as sprinklers, drip and SDI, efficiencies greater than 90% have been achieved, and are other strategies that can enhance WUE [10]. SDI has been used in recent years. It results in almost zero soil evaporation, high WUE, minimal deep percolation, optimum fertilizer supply, and increased crop productivity compared with other irrigation methods, including surface drip irrigation [13,14]. A significant factor affecting the amount of water plants can obtain from the soil is its ability to hold water. Understanding vertical and horizontal water movement is essential for crop production with respect to conserving water, and reducing N_2O and CO_2 emissions, as well as increasing yield [15]. Arif et al. [16] reported improved water retention in soils due to increased porosity after biochar amendment. Research has shown that adding biochar to soil increases its ability to hold water and reduces the need for irrigation [16,17].

The C content of biochar increases with an increasing carbonization temperature. pH increased considerably with a carbonization temperature from 300 °C to 550 °C then increased slowly when the carbonization temperature was over 550 °C [18]. Biochar's carbon content increases as pyrolysis temperature rises, while nitrogen (N) content decreases [19]. The high organic C content in biochar could increase CO_2 flux from the soil [20]. Reducing CO_2 emission from soils by biochar requires high soil organic matter OM content to increase dissolved organic carbon sorption [21,22]. With increasing pyrolysis temperatures, biochar's carbon and ash contents increase. In contrast, low-temperature biochar produces greater carbon and nutrient recovery, which is usually lost at higher temperatures [23]. The greatest biochar-induced carbon dioxide emissions were mainly found in low-temperature biochar samples, and decreasing emissions with increasing pyrolysis temperatures [24].

The production of vegetables is a crucial agricultural aspect in China [25]. Vegetables have recently become the primary crops grown in China due to their high economic value for farmers and health benefits. Chinese cabbage, also known as pakchoi cabbage (*Brassica rapa* L. ssp. Chinensis), is an important vegetable cultivated in south and northeast Asia and accounts for 30% to 40% of China's crop cultivation. It can be grown throughout the year and has lower production costs than other vegetable crops due to its simple seed production and short crop duration [26].

The influence of biochar addition on soil CO_2 and N_2O emissions has been thoroughly studied. However, to our knowledge, the effect of C content in wheat straw biochar under different SDI depths on soil CO_2 and N_2O fluxes, and plant growth performance and yield, have not been investigated. Based on the above, our study aimed to (a) assess the response of soil N_2O and CO_2 emissions to different C-content biochar, (b) determine the optimal depth of subsurface drip irrigation for high-efficiency gas mitigation while maintaining a high plant yield, and (c) investigate how different biochar C contents affect the growth and yield of pakchoi cabbage.

2. Materials and Methods

2.1. Description of Study Side and Experimental Setup

The experiment was carried out in a greenhouse under natural light conditions on *Brassica rapa* L. ssp. *Chinensis* at Hohai University, Jiangsu province, Gulou district, which is located in the central part of Nanjing City (31°95′ N, 118°83′ E), China, at a downstream area of the Yangtze River basin with an average elevation of 15 m above the sea level (Figure 1). Nanjing has multiple river systems, lakes, flatlands, and low hills. The weather on this side is humid subtropical under the influence of the East Asia Monsoon. Jiangsu is one of China's 13 main agricultural regions due to its geographic location, water availability, and historic farming practices. The average annual temperature is 16.5 °C, the absolute

maximum temperature reaches 43 °C in July, and the absolute minimum temperature drops to −16.9 °C in winter in January. July through September is the rainy season, the average annual rainfall is 1073 mm, and the average pan evaporation is 900 mm. Mean monthly climate record is listed in Table 1. The soil at the experimental site is yellow-brown with clay loam, it has a low organic matter content and is acidic. The chemical and physical properties of the soil are listed in Table 2. Crops in this region are important to the local economy because they create jobs, provide food, and help the province grow and develop. Rice, wheat, corn, soybeans, vegetables, and fruits are mainly produced in this area. Both the domestic market and international trade depend on these crops. The impact of these crops on the socio-economic development of Nanjing is significant. They offer farmers and farmworkers job opportunities. They have played a key role in the city's socio-economic development, contributing to poverty reduction, economic growth, and improved living standards.
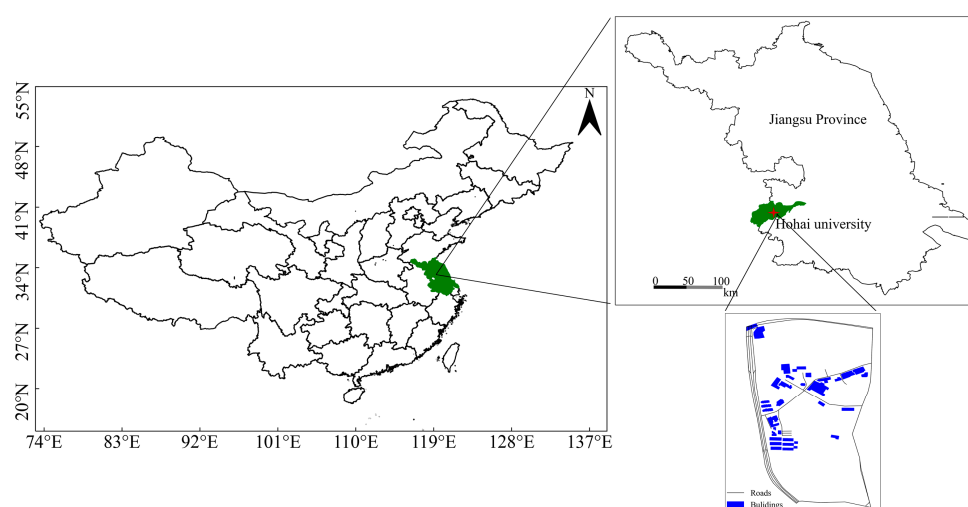

Figure 1. Location of the study area.

Table 1. Mean monthly climate record.

Parameter	2021											
	January	February	March	April	May	June	July	August	September	October	November	December
RH (%)	75.19	78.62	78.5	74.81	75.31	76.94	86.00	85.62	82.88	80.25	75.38	71.75
Max. T (°C)	16.37	24.24	26.01	30.16	33.57	34.4	34.84	32.98	32.76	34.17	23.57	17.3
Min. T (°C)	−9.86	−3.88	−2.46	3.93	11.37	16.00	22.31	20.4	15.9	5.9	−2.38	−5.59
Max. W (m/s)	6.86	8.68	7.29	9.28	7.80	8.02	8.00	4.78	6.49	8.13	9.00	7.89
Min. W (m/s)	0.14	0.25	0.22	0.24	0.22	0.09	0.12	0.09	0.06	0.33	0.09	0.35

Note: Meteorological date from NASA. https://power.larc.nasa.gov/data-access-viewer/ (accessed on 7 March 2023). RH relative humidity, Max. T: maximum temperature, Min. T: minimum temperature, Max. W: maximum wind speed, Min. W: minimum wind speed.

Table 2. Soil and biochar properties.

Property	Soil	Biochar
BD	1.35 g cm^{-3}	-
Soil porosity	0.33 g kg^{-1}	-
Silt	34.68%	-
Clay	43.59%	-
Sand	20.61%	-
pH	6.13	8.32
TN	1.32 g kg^{-1}	1.27
TP	0.23 g kg^{-1}	2.31
EC	0.38 ds m^{-1}	0.08

Note: BD: Bulk density, TN: total nitrogen, TP: total potassium, EC: electric conductivity.

The experimental design comprised a factorial combination of three subsurface drip irrigation depths, with subsurface drip irrigation emitters buried at 0.05 m (SDI$_5$), 0.10 m

(SDI$_{10}$), and 0.15 m (SDI$_{15}$), and three levels of C content in wheat straw biochar named no biochar (CK), low C content biochar (50% C=L), and high C content biochar 95% C=H). A completely randomized block design was used. Each treatment was repeated thrice, resulting in 27 pots (3 × 3 × 3 = 27 (Figure 2a)). For each pot, approximately 10 kg of the air-dried soil was mixed thoroughly with biochar to obtain a homogeneous mixture and achieve the desired application rate. The soil-biochar mixture was then poured into PVC pots with dimensions of 0.40 m length, 0.30 m width, and 0.20 m height, as shown in Figure 2b.
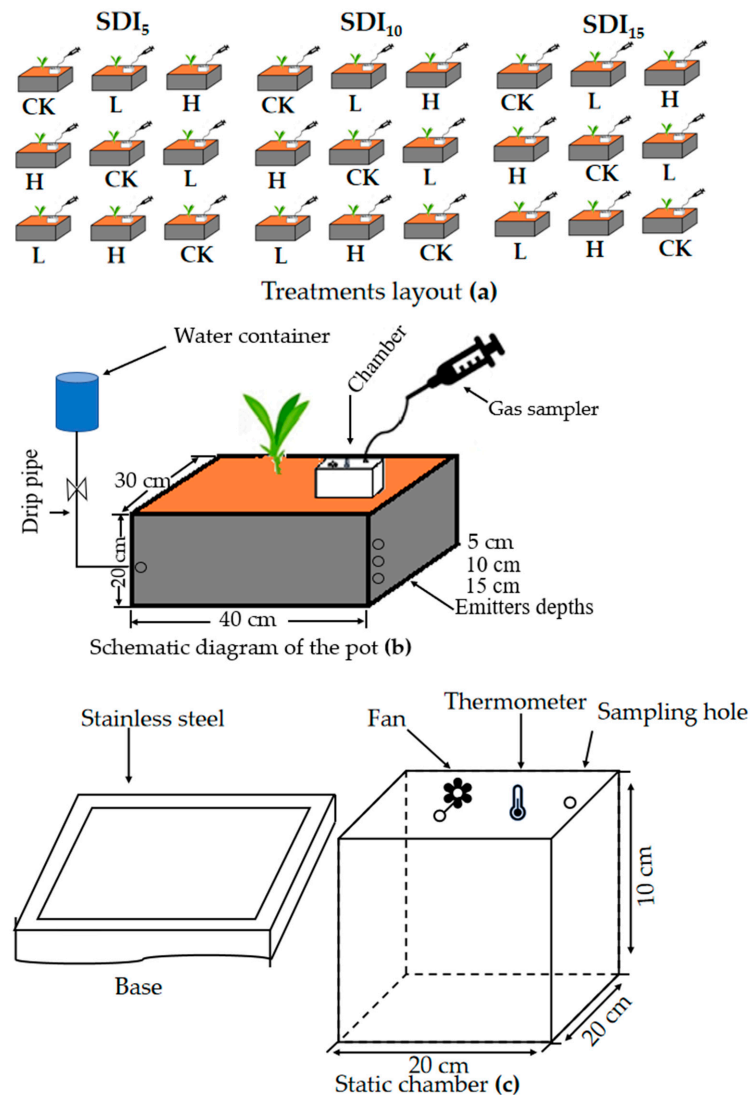

Figure 2. Experimental layout and treatments. Treatment layout (**a**), schematic diagram of the pot (**b**), and static chamber (**c**). CK: no biochar. L: low carbon content biochar. H: high carbon content biochar. SDI$_5$, SDI$_{10}$, and SDI$_{15}$ represent subsurface drip irrigation with drippers at 0.05, 0.10, and 0.15 m depths, respectively.

2.2. Soil Sampling and Analyses

Using a hand auger with a diameter of 0.05 m, 20 to 30 g of soil samples from various depths were collected (0.05–0.20 m). The soil samples were dried using an oven at a temperature of 105 °C for 24 h to determine the soil moisture content (θ) [27]. To calculate water-filled pore space (WFPS), the volume of gravimetric water was divided by the total porosity of the soil. The total porosity of the soil was calculated by determining the bulk density of the soil using the following equation:

$$\phi = 1 - \frac{BD}{PD} \tag{1}$$

where *BD* represents the bulk density and *PD* the particle density. The *PD* was 2.65 g cm^{-3} [28]. The following formula was used to convert the measured soil moisture into *WFPS*:

$$WFPS = \left(\text{VWC} \div \left(1 - \frac{BD}{2.65} \right) \right) \times 100\% \tag{2}$$

where: *VWC* is the volumetric water content.

Further 20–30 g soil samples were collected and dried at room temperature to determine physiochemical soil properties. The samples were dried by air, filtered (2 mm and 1 mm, respectively, for soil pH and electrical conductivity (EC)), blended with deionized water (soil water ratio = 1:2.5 and 1:5), agitated for three minutes, then left to stand three minutes. A pH meter (PHS-3E, China, Shanghai) and an electrical conductivity meter (TES-1381K, Taiwan) were used to measure pH and EC, respectively [29]. The soil was digested with H_2SO_4-H_2O_2, and the TN and TP were measured by spectrophotometer (UV1901, Kejie, Nanjing, China) [30].

2.3. N_2O and CO_2 Measurement and Analyses

Before running the experiment, a stainless-steel chamber base was inserted into each pot at a depth of about 0.05 m. The bases were left open throughout the experiment except when gas measuring. The bases were used to reduce lateral gas diffusion. The polyvinyl chloride chambers (length, width, and height = 0.20, 0.20, and 0.10 m) were equipped with thermometers (Figure 2c). The chambers were sealed by inserting them into stainless steel rings that were buried in the soil. A thermometer and an electric fan were included in the sampling chamber to monitor and mix the air temperature. To minimize the impact of heat transmission caused by ambient temperature, the chambers were covered in a heat isolation system. The chambers were immediately removed from their bases following gas sampling to prevent soil temperature, soil moisture, and microclimate alteration during the sampling.

N_2O and CO_2 were collected using 10-mL syringes connected to the chambers using a valve and pipe technique. N_2O and CO_2 samples were taken between 10:00~10:30 a.m. At 15-min intervals, three gas samples were taken from each chamber. Thermometers of 0.1 °C accuracy were used to measure the chamber air temperatures during each sampling. An electron capture detector (ECD) was used in a gas chromatograph (GC) (Agilent 7890A, Santa Clara, CA, USA) to monitor N_2O. A thermal conductivity detector (TCD) was used to determine the CO_2. The GC had a 30 m PoraPLOT-U column that separated N_2O and CO_2 from total gases at 36 °C. The gas fluxes were calculated by the linear regression slope of the time and the gas concentration using Formula (3) [31].

$$F = \rho.H.\frac{273}{273+T}.\frac{dc}{dt} \tag{3}$$

where *F* stands for gas flux (μg m^{-2} h^{-1}), ρ for the gas density (1.973 kg m^{-3}), *H* for the chamber's height (m), *T* for the chamber's mean air temperature (°C), and dC/dt for the linear rate of increase in gas concentration over time (μL m^{-3} h^{-1} for N_2O and mL m^{-2} h^{-1} for CO_2). Daily fluxes throughout the study period were integrated to obtain the cumulative emissions of N_2O and CO_2.

2.4. Agronomic Practices and Growth Indicator Measurements

The biochar used in this work was wheat straw biochar with a pyrolysis temperature of 500–600 °C purchased with different C contents from Sanli New Energy factory, Henan Province, China, and was used at a rate of 5%, equivalent to 500 g/10 kg of the clay loam soil. Seeds of pakchoi cabbage (*Brassica rapa* L. ssp. Chinensis) were directly sown into the experimental pots. A gravity drip system with a discharge controller was used to

supply irrigation water to the pots (Figure 2b). Each pot had a separate drip line. The plants received three irrigations with two-week irrigation intervals (winter season). Urea-based nitrogen fertilizer (N > 46.2%, Jiangsu Huachang Chemical Company, Zhangjiagang, China) was applied once with irrigation water as fertilizer at the recommended dosage of 300 kg N ha^{-1}. Insects and weeds were controlled whenever necessary.

Three plants were selected in every treatment to measure growth indicators. A 100 cm stainless steel ruler was used to measure plant height (PH) and leaf number at 10-day intervals. PH was measured from the soil surface to the highest top leaf of the plant. Leaf area index was determined by applying a total green leaf area to the number of plants in a square meter. Pakchoi parts were divided into roots and leaves and weighed separately. On the harvesting day, the root length was determined using a 100 cm stainless steel ruler after being washed free of soil particles. Plant shoot and root biomass were obtained by oven drying at 70 °C.

2.5. Statistical Analysis

Before analysis of variance, all data were checked for normality and homogeneity of variance using Skewneses and Kurtoses and Levene's tests, and were found to have a normal distribution; thus, no transformation was necessary. An IBM-SPSS (19, Chicago, IL, USA) was carried out used to analyze the data. Two-way analysis of variance was conducted to determine if the variations between treatments were significant at the 0.05 significance level. When the F-test was statistically significant ($p \leq 0.05$), mean comparisons were made using Duncan's multiple range test at the 0.05 probability level. Surfer software (Golden Software Inc., Golden, CO, USA) was utilized to generate the figures for the distribution of soil moisture (Figure 3). GraphPad Prism 8.0.2 was used to draw the other figures.
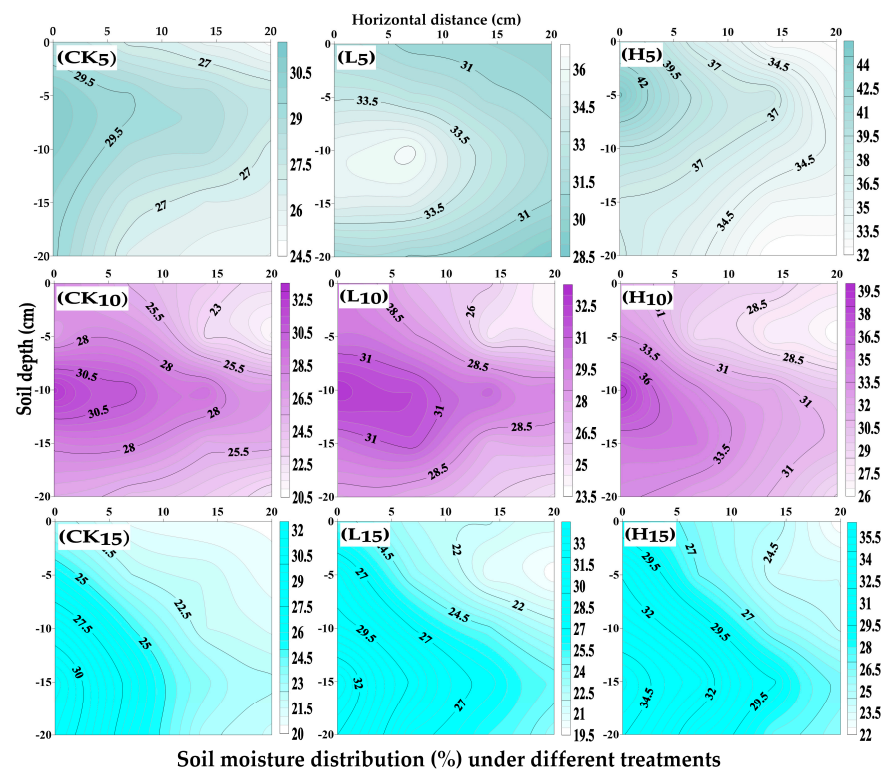

Figure 3. Vertical and horizontal soil moisture dynamic under different irrigation depths, and C content in biochar. CK: no biochar. L: Low carbon content biochar. H: high carbon content biochar. The subscript numbers 5, 10, and 15 represent subsurface drip irrigation with drippers buried at 0.05, 0.10, and 0.15 m depths, respectively.

3. Results

3.1. Wetting Pattern Dynamics

As shown in Figure 3, vertical and horizontal soil moisture distribution gradually decreased with increasing the distance from the emitter. Across different subsurface drip irrigation (SDI) depths, soil moisture level under SDI_5 was higher than levels under SDI_{10} and SDI_{15}, with the water moving more quickly downward than upward. Within each SDI depth, the carbon content (C) in the biochar significantly affected soil moisture distribution. High C biochar (H) increased soil moisture, followed by low C biochar (L) and control (CK). Table 3 shows that the mean soil moisture distribution significantly increased as irrigation depth decreased. The maximum soil moisture of 35.97% was seen under SDI_5, whereas the minimum was 24.02% under SDI_{15}. Under each SDI depth, the soil moisture increased as the C content in the biochar increased. Compared to CK, L and H increased soil moisture by (15.42, 29.54%), (7.60, 19.95%), and (6.41, 18.07%) for SDI_5, SDI_{10}, and SDI_{15}, respectively.

Table 3. Mean and standard deviation of the soil moisture content overall experimental period.

Irrigation Depth (m)	C Content in Biochar	Mean Soil Moisture Content (%)
SDI_5	CK	27.77 ± 1.2 [Ac]
	L	32.05 ± 1.3 [Ab]
	H	35.97 ± 1.5 [Aa]
SDI_{10}	CK	26.17 ± 1.1 [Bc]
	L	28.16 ± 1.2 [Bb]
	H	31.39 ± 1.3 [Ba]
SDI_{15}	CK	24.02 ± 1.0 [Cc]
	L	25.56 ± 1.1 [Cb]
	H	28.36 ± 1.2 [Ca]

Note: SDI_5, SDI_{10}, and SDI_{15} represent subsurface drip irrigation in which drippers are buried at 0.05, 0.10, and 0.15 m depths, respectively. CK, L, and H represent no, low, and high carbon content biochar, respectively. Uppercase and lowercase letters above the means denote significant differences according to Duncan's multiple range test at the 0.05 significance level.

3.2. Nitrous Oxide (N_2O) Flux

Apparent increases in N_2O fluxes appeared in a short period after irrigation. Regardless of the C content of the biochar, the highest peaks of the N_2O fluxes (28.85, 32.18, and 29.95 $\mu g\ N_2O\ m^{-2}\ h^{-1}$) occurred 72 h after the first irrigation for SDI_5, SDI_{10}, and SDI_{15}, respectively, then the N_2O flux began to reduce gradually until the end of the experiment (Figure 4a–c). Within each of the three SDI depths, N_2O flux decreased with increasing C content in biochar. Under the SDI_5 treatment (Figure 4a), the peaks of N_2O fluxes were 28.85, 24.86, and 22.94 $\mu g\ N_2O\ m^{-2}\ h^{-1}$ for CK, L, and H, respectively, for SDI_{10} they were 32.18, 24.27, and 25.86 $\mu g\ N_2O\ m^{-2}\ h^{-1}$ (Figure 4b), and for the SDI_{15} were 29.95, 27.82, and 24.28 $\mu g\ N_2O\ m^{-2}\ h^{-1}$ (Figure 4c) corresponding to CK, L, and H. ANOVA results revealed that there was a significant interaction effect between irrigation depth and C content in biochar, which decreased N_2O emissions under high C with SDI_5.

3.3. Carbon Dioxide (CO_2) Flux

CO_2 emissions were variable during the growing season, ranging from 351.04–33.90 $\mu g\ CO_2\ m^{-2}\ h^{-1}$. As presented in Figure 4d–f, the fluctuation in the soil CO_2 flux at every irrigation depth followed the same trend. Throughout the experimental period, the peak value of the CO_2 flux at each irrigation depth was mainly concentrated at the beginning of the experiment at 72 h after the first irrigation (Figure 4d–f). Among the three irrigation depths, the highest mean CO_2 flux was at SDI_{15} (246.66 $\mu g\ CO_2\ m^{-2}\ h^{-1}$), followed by SDI_{10} (169.07 $\mu g\ CO_2\ m^{-2}\ h^{-1}$) and SDI_5 (168.41 $\mu g\ CO_2\ m^{-2}\ h^{-1}$). Under each SDI treatment, the CO_2 flux decreased significantly as the C content in biochar increased (Figure 4d–f). Compared to the CK, the L and H treatments showed decreased CO_2 flux by (8.05, 31.46%), (6.96, 28.88%),

and (2.97, 7.89%) for SDI_5, SDI_{10}, and SDI_{10}, respectively. ANOVA indicated that SDI_{15} significantly increased CO_2 flux, whereas no significant effect between SDI_5 and SDI_{10} was detected. Due to the significant interaction effect, the combination of the irrigation depth and C content reduced CO_2 emissions while irrigation depth with CK increased emissions.
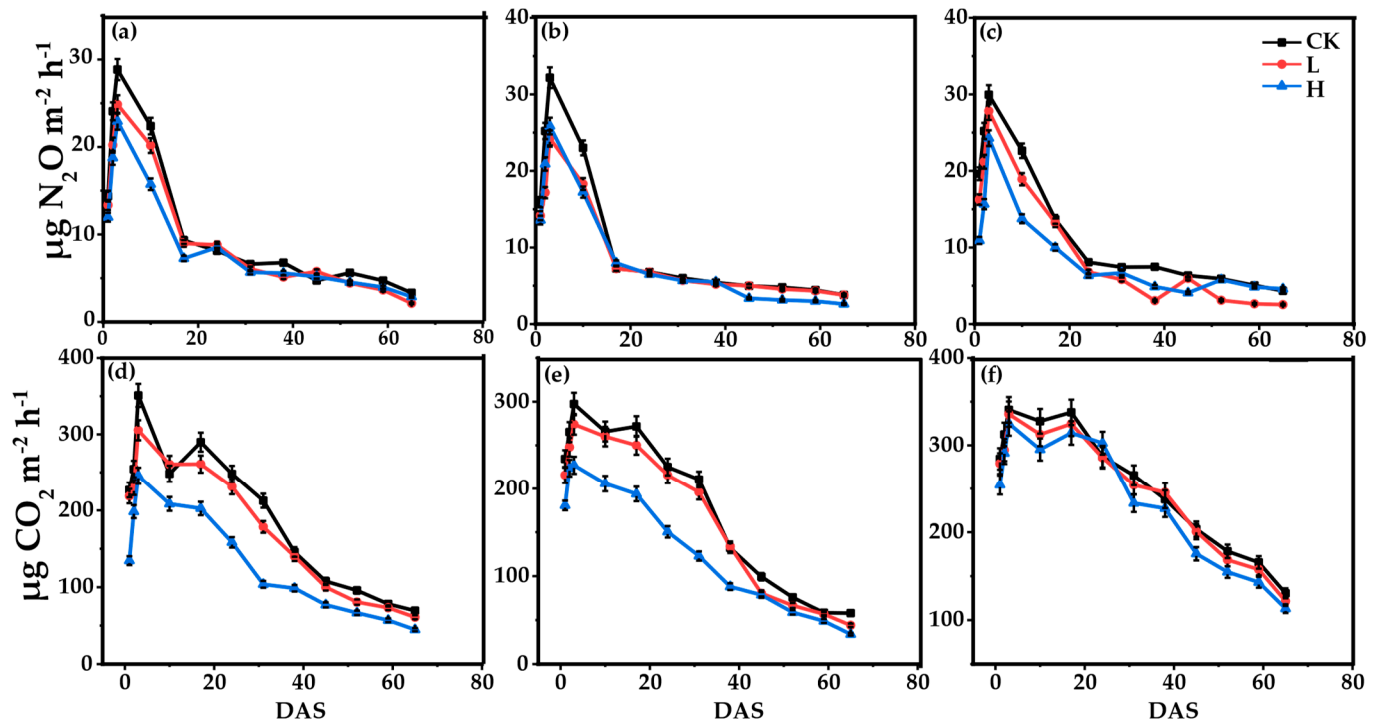

Figure 4. The trend of N_2O and CO_2 fluxes under different subsurface drip irrigation depths SDI_5 (**a**,**d**), SDI_{10} (**b**,**e**), and SDI_{15} (**c**,**f**), and different C content in biochar. CK, L, and H represent no, low, and high carbon content biochar, respectively. DAS means days after sowing.

3.4. Cumulative N₂O and CO₂ Emissions

The cumulative N_2O flux over the whole experimental period at the three irrigation depths and different biochar C contents are shown in Table 4. The highest cumulative values of N_2O emissions were obtained under SDI_{15}, but no significant differences occurred between the three SDI treatments. Increasing the C content from zero (CK) to high significantly reduced N_2O emissions within the sub-treatments, as shown in Table 4. Compared to the control treatment (CK), the L and H treatments decreased the N_2O fluxes by (17.46, 29.87%), (0, 27.91%), and (8.20, 19.60%) under SDI_5, SDI_{10}, and SDI_{15}, respectively.

Table 4. Cumulative N_2O and CO_2 emissions over the whole experimental period.

	Treatment	CK	L	H
N_2O (mg N_2O m^{-2})	SDI_5	7.82 ± 0.24 [Ba]	7.18 ± 0.22 [Bb]	6.13 ± 0.19 [Bc]
	SDI_{10}	8.74 ± 0.27 [ABa]	8.74 ± 0.20 [ABb]	6.30 ± 0.20 [ABc]
	SDI_{15}	8.74 ± 0.27 [Aa]	7.21 ± 0.23 [Ab]	6.28 ± 0.20 [Ac]
CO_2 (mg CO_2 m^{-2})	SDI_5	147.23 ± 7.70 [Ba]	137.69 ± 7.20 [Ba]	101.82 ± 5.33 [Bb]
	SDI_{10}	141.38 ± 7.40 [Ba]	133.24 ± 6.97 [Ba]	100.07 ± 5.23 [Bb]
	SDI_{15}	191.77 ± 10.03 [Aa]	186.33 ± 9.75 [Aa]	178.20 ±9.32 [Ab]

Note: SDI_5, SDI_{10}, and SDI_{15} represent subsurface drip irrigation with drippers buried at 0.05, 0.10, and 0.15 m below the soil surface. CK, L, and H represent no, low, and high carbon biochar content, respectively. Uppercase and lowercase letters above the means indcate significant differences according to Duncan's multiple range test at the 0.05 significance level.

As shown in Table 4, the cumulative CO_2 flux over the study period increased with irrigation depth. SDI_{15} had the highest cumulative CO_2 emissions among different irrigation depths, while no significant differences were noticed between SDI_5 and SDI_{10} treatments. Regardless of irrigation depth, the cumulative CO_2 emissions at different C contents in biochar were from high to low as follows: CK > L > H (Table 4). Compared to the control treatment (CK), the CO_2 emissions of the L and H treatments decreased by (6.48, 30.84%), (5.76, 29.22%), and (2.84, 7.07%) under SDI_5, SDI_{10}, and SDI_{15}, respectively.

3.5. Growth Parameters and Yield Traits

3.5.1. Plant Height (PH), Leaf Area Index (LAI), Leaves Number (LN), and Maximum Root Length (MRL)

Compared with CK, applying different C-content biochar under different SDI depths significantly affected crop growth performance. Among the three SDI depths, SDI_5 had the highest values of PH, followed by SDI_{10} and SDI_{15} (Figure 5a). Within individual SDI treatments, compared to the CK, L and H significantly increased PH by (23.29, 41.05%), (29.56, 48.67%), and (18.93, 40.88%) for SDI_5, SDI_{10}, and SDI_{15}, respectively.

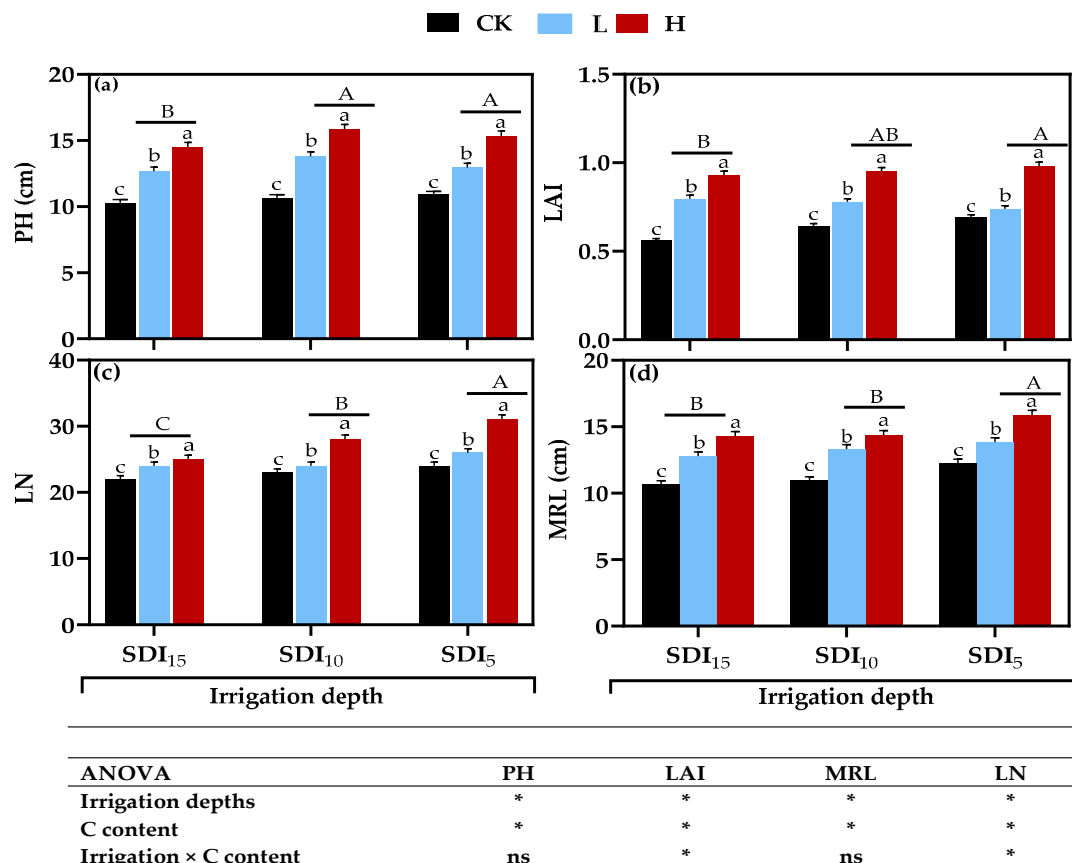| ANOVA	PH	LAI	MRL	LN
Irrigation depths	*	*	*	*
C content	*	*	*	*
Irrigation × C content	ns	*	ns	*

Figure 5. Plant height (**a**), leaf area index (**b**), leaf number per plant (**c**), and maximum root length (**d**) under different irrigation depths and C content in biochar. CK, L, and H represent no, low, and high carbon content biochar, respectively. Uppercase and lowercase letters above the grouped column and the error bars indicate significant differences according to Duncan's multiple range test at the 0.05 significance level. * denotes significant at ($p \leq 0.05$) level, and ns denotes not significant. PH, LAI, LN, and MRL represent plant height, leaf area index, leaf number, and maximum root length, respectively.

The effects of different irrigation depths, different biochar C-content, and their interactions on LAI, were significant. As shown in Figure 5b, the maximum LAI was noticed in SDI_5, followed by SDI_{10} and SDI_{15}. Under the same irrigation depth, and compared to

CK, the L and H treatments significantly increased LAI, with the order H > L > CK. The same trend was observed for all three SDI treatments. Due to the interaction effect, the high C biochar under the SDI_5 treatment had the maximum LAI, whereas the minimum was under SDI_{15} with CK (Figure 5b).

The application of different C-content biochar under different SDI depths and their interaction significantly influenced the leaf number of pakchoi cabbage. As presented in Figure 5c, the maximum number of leaves per plant occurred in the SDI_5 treatment, whereas the minimum occurred in SDI_{15}. Within each SDI treatment, the maximum leaf number per plant was observed under the H treatment, followed by L and CK treatments. The same pattern was seen in all SDI treatments. At the same irrigation depth, the number of leaves per plant increased significantly as the C content in the biochar increased, with the H treatment having the most and CK having the least. Because of the interaction effect between irrigation depth and C content in the biochar, the combination of SDI_5 and high C content biochar outperformed the other treatments.

ANOVA results showed significant differences among SDI treatments. SDI_5 had the longest maximum root length, followed by SDI_{10} and SDI_{15} (Figure 5d). In the same irrigation depth with different biochar C content, the H and L treatments had higher maximum root lengths compared to CK. For example, SDI_5 resulted in 15.95, 13.83, and 12.25 cm for H, L, and CK, followed by SDI_{10} (14.37, 13.33, and 10.98 cm), SDI_{15} (14.30, 12.79, and 10.69 cm) for H, L, and CK, respectively.

3.5.2. Aboveground Biomass (AGB), Root Dry Biomass (RDB), Aboveground Weight (AGW), and Root Fresh Weight (RFW)

The application of different C-content biochar under different SDI depths significantly ($p \leq 0.05$) affected the aboveground biomass. At the three irrigation depths, SDI_5 significantly increased AGB, followed by SDI_{10} and SDI_{15} (Figure 6a). Under each of the three irrigation depths, the mean AGB significantly ($p \leq 0.05$) increased with the increasing the amount of the C content in biochar. Under SDI_5 14.03, 11.88, and 9.44 g plant^{-1} were recorded for the H, L, and CK, respectively, followed by SDI_{10} 9.86, 9.25, and 7.25 g plant^{-1}, whereas the lowest values of 8.80, 8.24, and 6.38 g plant^{-1} were observed in SDI_{15} (Figure 6a).

Similar to aboveground biomass, RDB was significantly influenced by the SDI depths and biochar C content, and their interaction. As presented in Figure 6b, among SDI treatments, the highest values of RDB occurred in the SDI_5 treatment, whereas the lowest values were seen in the SDI_{15} treatment. Within individual SDI treatments, the RDB significantly varied with C content in the biochar. Compared to the CK, the L and H increased RDB by (49.05, 83.63%), (47.68, 88.92%), and (57.98, 74.32%) under SDI_5, SDI_{10}, and SDI_{15}, respectively. The ANOVA results indicate a significant interaction between irrigation depth and different C-content biochar.

Figure 6c shows that the effects of SDI depths and different biochar C contents on aboveground weight (yield) were significant ($p \leq 0.05$). AGW increased significantly in the order $SDI_5 > SDI_{10} > SDI_{15}$. For the same irrigation depth, compared to CK, the H and L treatments under the SDI_5 treatment resulted in a maximum AGW of 130.84 and 121.65 g plant^{-1}, respectively, and the minimum 92.34 and 84.52 g plant^{-1} were observed in the SDI_{15}.

Analysis of variance indicates that the highest mean RFW occurred in SDI_5 compared to other treatments, whereas no significant differences ($p \geq 0.05$) were detected between SDI_{10} and SDI_{15} (Figure 6d). Within the same irrigation depth, RFW tended to increase with the C content in biochar. The highest values were observed in the H treatment, followed by L and CK (Figure 6d). The interaction of SDI depth and different biochar C contents significantly affected the AGB, which led to high C biochar under SDI_5 treatment having the highest values. CK under SDI_{15} had the lowest values.
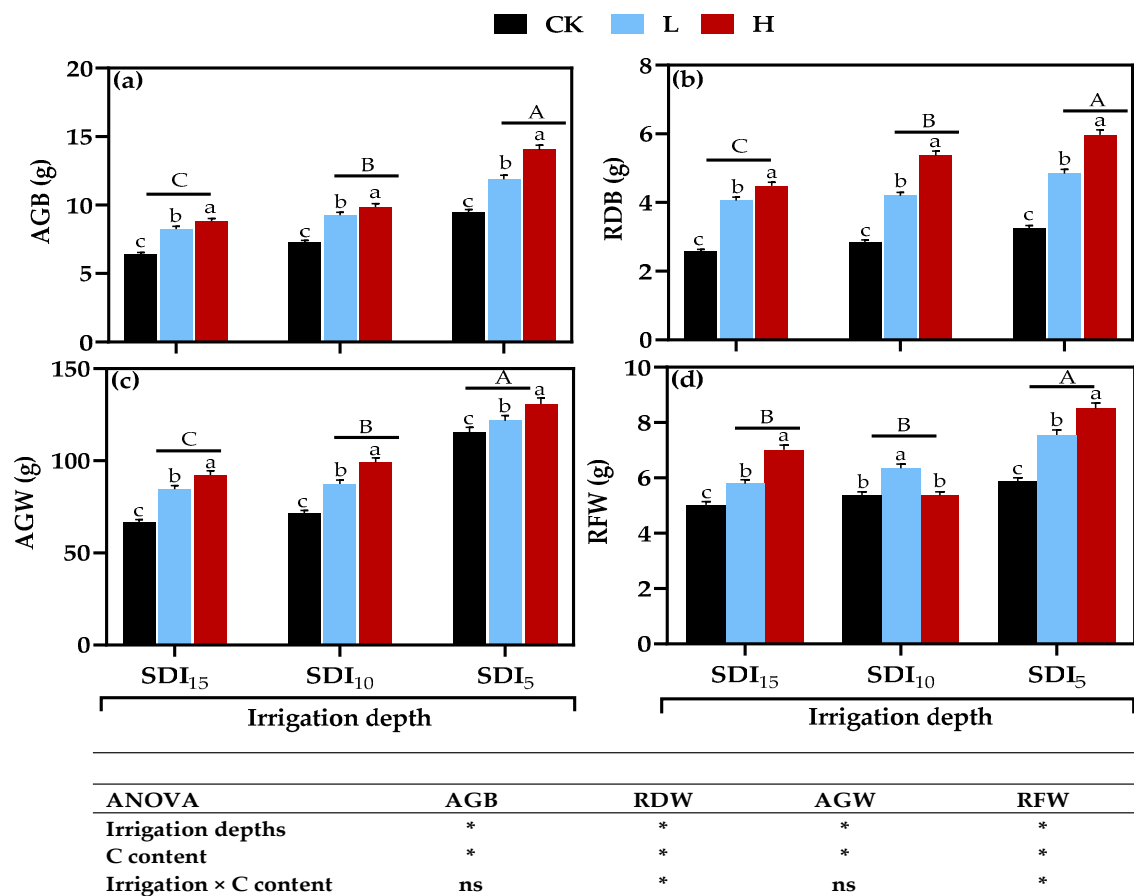
ANOVA	AGB	RDW	AGW	RFW
Irrigation depths	*	*	*	*
C content	*	*	*	*
Irrigation × C content	ns	*	ns	*

Figure 6. Aboveground biomass (**a**), root dry biomass (**b**), aboveground weight (**c**), and root fresh weight (**d**) under different irrigation depths and biochar C content. CK, L, and H represent no, low, and high carbon content biochar, respectively. Uppercase and lowercase letters above the grouped column and the error bars indicate differences according to Duncan's multiple range test at the 0.05 significance level. * denotes significant at ($p \leq 0.05$) level, and ns denotes not significant. AGB, RDB, AGW, and RFW represent aboveground biomass, root dry biomass, aboveground weight, and root fresh weight, respectively.

4. Discussion

4.1. The Effect of Different Biochar C Contents and Irrigation Depths on Soil Moisture Dynamics

Water distribution in the soil profile is presented by contour maps in Figure 3. Irrigation depths significantly affected the soil moisture distribution. The soil moisture peaked after irrigation and then gradually decreased until the following irrigation period, with the SDI_5 treatment having the highest soil moisture content. Soil moisture content declined as the lateral distance from the emitter increased [32]. The soil moisture distribution changed quickly after watering as water moved rapidly through the soil and then slowed down [32]. In the current study, soil moisture decreased as the horizontal distance increased from the emitter point. This is consistent with Kuang et al. [33], who concluded that soil moisture in areas away from the drip point would likely be even lower, limiting nitrification and denitrification processes. Similarly, Wei et al. [27] reported soil moisture decreased gradually in a horizontal direction with increasing radial distance to the emitter. The decrease in microbial activity with the reduction in soil moisture resulted in less gas emission. Nitrification is an important source of N_2O released from the soil at low soil water contents [34]. As shown in Figure 3, in the vertical direction, soil moisture decreased as depth increased. Our findings are consistent with Weldon et al. [35], who stated that soil moisture and the soil matrix's depletion eventually decreased microbial activity, and thus, emissions. Biochar has been proposed as a potential substance for soil amendment to enhance soil moisture

retention, soil structure, soil C storage, and greenhouse gas emissions (GHGs) [36]. Adding biochar to the soil increases its water-holding capacity and improves aeration [37,38]. In the current study, compared to the control (CK), L and H carbon content biochar increased soil moisture by (15.42, 29.54%), (7.60, 19.95%), and (6.41, 18.07%) for SDI_5, SDI_{10}, and SDI_{15}, respectively, indicating that C content has a significant effect on soil moisture retention and soil moisture increases with C content increase. This is due to the increase in carbonization temperature during biochar production, which results in the C particles being crushed, the average pore size and soil bulk density decreasing, and micropores being formed. When micropores are small, they help retain moisture for a long time. These findings are in line with results of several studies. For example, Zhao et al. [39] reported that adding biochar impacts soil moisture content, probably due to hydrophilic domains, high porosity, and the high surface area of biochar. The pyrolysis temperature of biochar affected soil water retention in [40].

4.2. N_2O Emissions Response to Irrigation Depths and Different C Content Biochar

In recent decades, GHG emissions from agricultural fields have received wide attention because of the fast development of intensive agriculture and a large amount of chemical fertilizer input. Biochar is a porous medium with a high surface area, and can absorb a significant amount of nitrous oxide when applied to soils [36,41]. Several recent studies indicate that biochar additions may reduce soil nitrous oxide (N_2O) emissions. For instance, Ref. [42] investigated the effect of biochar application on greenhouse gas emissions and soil C sequestration in corn cultivated under subsurface drip irrigation (SDI). It was found that N_2O flux could be reduced compared to the control treatment because of an increase in soil pH by adding biochar, which stimulates N_2O emissions, direct N_2O adsorption promoted by the high specific surface area of biochar, and changes in microbial community structure. In our study, biochar-amended soils emitted less N_2O than the control, and N_2O emission occurred immediately following irrigation, then decreased gradually. This can be explained by the fact that the rapid alternation between wetting and drying after irrigation stimulates microorganism activity in the soil and nitrogen (N) transformation, resulting in greater N_2O emissions [43]. Therefore, microbial activity eventually decreased due to the decline in soil moisture and the consumption of soil N, which reduced the emissions. In the current study, we noticed N_2O flux under SDI with high C content biochar (SDI_5 + H) was significantly less than in other treatments (Figure 4a–c). This phenomenon could be explained by emitters being buried at 5 cm with soil layers below 5 cm being wet, and the soil layers above gradually drying. The wetted part of the soil would be greater than the dry part, and oxygen diffusion decreased, which promotes the best conditions for biochar to dissolve into the soil and create good conditions for plant roots to uptake water and nutrients; thus, the emission was reduced. Another reason could be that the high biochar C-content decreased soil bulk density and enhanced its capacity for absorbing moisture. In general, in our study, gas emissions were low because winter temperatures were lower than those of the other seasons; various microorganisms' activities in the soil were decreased, which decreased the soil respiration rate.

4.3. CO_2 Emission Response to Irrigation Depths and Different Biochar C Content

The increase in C content obtained by adding biochar to the soil stimulates the humification and C storage processes and improves soil density and water retention [6,44]. Biochar amendment effectively reduced CO_2 release and increased organic C content compared to control soil [45]. In our study, CO_2 emissions peaked within three days of irrigation and then gradually decreased (Figure 4d–f). The CO_2 flux was higher for the control than for both different C-content biochar treatments, indicating that biochar amendment suppressed CO_2 emissions. Adding biochar to the soil significantly decreased soil mineralization, which was the primary source of CO_2 emissions [46,47].

Compared to CK, the L and H treatments significantly decreased CO_2 emissions; among L and H treatments, CO_2 emissions under L were higher than under H. One

possible explanation for these results is that the biochar used in L was produced at low temperatures. Thus, it could have contained many unstable materials such as cellulose, hemicellulose, and other complex carbohydrates. These materials are also partially used by microorganisms, subsequently increasing soil carbon dioxide emissions. Our findings were consistent with Lahijani et al. [48], who reported that biochar made at high pyrolysis temperatures has a more substantial carbon dioxide capture effect. This is because as carbonization temperature increases, the carbon particles are crushed, the average pore size decreases, and micropores form.

4.4. Influence of Irrigation Depths and Different Biochar C Content on Plant Growth and Yield

Biochar addition to soil would increases plant access to readily available micronutrients [49]. Improving the soil's chemical, physical, and biological properties enhances plant growth and productivity by increasing the quantity and availability of nutrient components, minimizing nutrient leaching, and decreasing gaseous component losses [9,50]. In the current study, the overall means of plant height (PH), leaf area index (LAI), leaf number (LN), and maximum root length (MRL) under SDI_5 were significantly ($p \leq 0.05$) greater compared to SDI_{10} and SDI_{15}. This indicates better conservation of soil moisture at this depth. In other words, the soil layers below 5 cm are wet. From 5 cm and above, layers are gradually dried, which means that the wetted part of the soil is greater than the dry part. Oxygen diffusion decreases, which promotes the best conditions for the biochar to dissolve into the soil and create the best conditions for roots to uptake water and nutrients. Regardless of the irrigation depths, the results showed that increasing the C content in biochar significantly ($p \leq 0.05$) increased all plant growth indicators.

Regardless of the C content of biochar, SDI_5 showed better results for aboveground biomass (AGB), root dry biomass (RDB), aboveground weight (AGW), and root fresh weight (RFW) relative to other irrigation depths. This could be due to better root distribution in this layer, which would allow roots to easily obtain water and nutrients because the soil is wet from 5 cm and below. In other words, almost the entire root zone is wet, and the root can easily obtain water compared to those at other depths. Roots, here, develop vertically rather than horizontally to obtain water and nutrients. The vertical roots fix and support the plant rather than provide nutrients. On the other hand, compared to the CK treatment, the AGB, RDB, AGW, and RFW significantly ($p \leq 0.05$) enhanced with the increase of C content in biochar. We postulate that this is because high C-content biochar was produced at a higher pyrolysis temperature than low C-content biochar and CK. Our results are supported by Biederman et al. [51], who stated that biochar made at higher temperatures was more efficient at promoting aboveground production, and a combination of suitable depth (SDI_5) and high C-content biochar gave a better performance, as in our study. The addition of biochar to agricultural production and GHG mitigation has been intensively studied, but the effects of wheat straw biochar properties, especially the carbon content of biochar under different subsurface drip irrigation depths on soil GHG emissions and crop production, have been rarely studied. To meet population growth demand, it is necessary to produce more food, and the balance between production and protection of the environment is important. Therefore, additional research is required to completely determine how biochar works to reduce the effects of climate change while enhancing crop productivity.

5. Conclusions

This study suggested that biochar had a sustainable positive effect on mitigating greenhouse gas emissions, enhancing crop productivity, and maintaining soil moisture retention. Compared to the no biochar treatment (CK), all plant growth indicators improved significantly with biochar-amended treatments. Increasing C content in biochar enhanced growth performance and plant productivity and reduced N_2O and CO_2 emissions. Biochar amendment had a considerable influence on soil moisture retention. The soil moisture content under the biochar-added treatments was significantly higher than in the no biochar

treatment, and soil moisture under high C biochar was greater than under low C biochar. As the lateral distance from the emitter increased, soil moisture decreased, and in the vertical direction it was reduced as depth increased. Biochar produced at high pyrolysis temperatures (>550 °C) can potentially mitigate N_2O and CO_2 emissions. In addition, irrigation depth was an important factor in this study, and significantly affected N_2O and CO_2 emissions and plant growth and yield. Thus, much more work should be put into developing high-efficiency solutions for reducing greenhouse gas emissions and improving agriculture productivity, as well as carefully evaluating the potential effects of biochar and its properties by biochar amendment.

References

1. Lehmann, J.; Gaunt, J.; Rondon, M. Bio-Char Sequestration in Terrestrial Ecosystems—A Review. *Mitig. Adapt. Strateg. Glob. Chang.* **2006**, *11*, 403–427. [CrossRef]
2. Zhang, Y.; Wang, J.; Feng, Y. The Effects of Biochar Addition on Soil Physicochemical Properties: A Review. *Catena* **2021**, *202*, 105284. [CrossRef]
3. Han, J.; Zhang, A.; Kang, Y.; Han, J.; Yang, B.; Hussain, Q.; Wang, X.; Zhang, M.; Khan, M.A. Biochar Promotes Soil Organic Carbon Sequestration and Reduces Net Global Warming Potential in Apple Orchard: A Two-Year Study in the Loess Plateau of China. *Sci. Total Environ.* **2022**, *803*, 150035. [CrossRef]
4. Cabeza, I.; Waterhouse, T.; Sohi, S.; Rooke, J.A. Effect of Biochar Produced from Different Biomass Sources and at Different Process Temperatures on Methane Production and Ammonia Concentrations in Vitro. *Anim. Feed Sci. Technol.* **2018**, *237*, 1–7. [CrossRef]
5. Liang, B.; Lehmann, J.; Sohi, S.P.; Thies, J.E.; O'Neill, B.; Trujillo, L.; Gaunt, J.; Solomon, D.; Grossman, J.; Neves, E.G.; et al. Black Carbon Affects the Cycling of Non-Black Carbon in Soil. *Org. Geochem.* **2010**, *41*, 206–213. [CrossRef]
6. Tomczyk, A.; Sokołowska, Z.; Boguta, P. Biochar Physicochemical Properties: Pyrolysis Temperature and Feedstock Kind Effects. *Rev. Environ. Sci. Biotechnol.* **2020**, *19*, 191–215. [CrossRef]
7. Xiao, X.; Chen, B.; Chen, Z.; Zhu, L.; Schnoor, J.L. Insight into Multiple and Multilevel Structures of Biochars and Their Potential Environmental Applications: A Critical Review. *Environ. Sci. Technol.* **2018**, *52*, 5027–5047. [CrossRef] [PubMed]
8. Kamali, M.; Sweygers, N.; Al-Salem, S.; Appels, L.; Aminabhavi, T.M.; Dewil, R. Biochar for Soil Applications-Sustainability Aspects, Challenges and Future Prospects. *Chem. Eng. J.* **2022**, *428*, 131189. [CrossRef]
9. Liu, X.; Zhang, J.; Wang, Q.; Shaghaleh, H.; Chang, T.; Hamoud, Y.A. Modification of Soil Physical Properties by Maize Straw Biochar and Earthworm Manure to Enhance Hydraulic Characteristics under Greenhouse Condition. *Sustainability* **2022**, *14*, 13590. [CrossRef]
10. Jovanovic, Z.; Stikic, R. Partial Root-Zone Drying Technique: From Water Saving to the Improvement of a Fruit Quality. *Front. Sustain. Food Syst.* **2018**, *1*, 3. [CrossRef]
11. Hamoud, Y.A.; Guo, X.; Wang, Z.; Chen, S.; Rasool, G. Effects of Irrigation Water Regime, Soil Clay Content and Their Combination on Growth, Yield, and Water Use Efficiency of Rice Grown in South China. *Int. J. Agric. Biol. Eng.* **2018**, *11*, 144–155. [CrossRef]
12. Carrijo, D.R.; Akbar, N.; Reis, A.F.B.; Li, C.; Gaudin, A.C.M.; Parikh, S.J.; Green, P.G.; Linquist, B.A. Impacts of Variable Soil Drying in Alternate Wetting and Drying Rice Systems on Yields, Grain Arsenic Concentration and Soil Moisture Dynamics. *F Crop. Res.* **2018**, *222*, 101–110. [CrossRef]

13. Fu, B.; Li, Z.; Gao, X.; Wu, L.; Lan, J.; Peng, W. Effects of Subsurface Drip Irrigation on Alfalfa (*Medicago Sativa* L.) Growth and Soil Microbial Community Structures in Arid and Semi-Arid Areas of Northern China. *Appl. Soil Ecol.* **2021**, *159*, 103859. [CrossRef]

14. Martínez-Gimeno, M.A.; Bonet, L.; Provenzano, G.; Badal, E.; Intrigliolo, D.S.; Ballester, C. Assessment of Yield and Water Productivity of Clementine Trees under Surface and Subsurface Drip Irrigation. *Agric. Water Manag.* **2018**, *206*, 209–216. [CrossRef]

15. Hamad, A.A.A.; Wei, Q.; Xu, J.; Hamoud, Y.A.; He, M.; Shaghaleh, H.; Wei', Q.; Li, X.; Qi, Z. Managing Fertigation Frequency and Level to Mitigate N_2O and CO_2 Emissions and NH_3 Volatilization from Subsurface Drip-Fertigated Field in a Greenhouse. *Agronomy* **2022**, *12*, 1414. [CrossRef]

16. Arif, M.; Ilyas, M.; Riaz, M.; Ali, K.; Shah, K.; Ul Haq, I.; Fahad, S. Biochar Improves Phosphorus Use Efficiency of Organic-Inorganic Fertilizers, Maize-Wheat Productivity and Soil Quality in a Low Fertility Alkaline Soil. *F. Crop. Res.* **2017**, *214*, 25–37. [CrossRef]

17. Güereña, D.; Lehmann, J.; Hanley, K.; Enders, A.; Hyland, C.; Riha, S. Nitrogen Dynamics Following Field Application of Biochar in a Temperate North American Maize-Based Production System. *Plant Soil* **2013**, *365*, 239–254. [CrossRef]

18. Liu, Z.; Niu, W.; Chu, H.; Zhou, T.; Niu, Z. Effect of the Carbonization Temperature on the Properties of Biochar Produced from the Pyrolysis of Crop Residues. *BioResources* **2018**, *13*, 3429–3446. [CrossRef]

19. Hui, D.; Hui, D. Effects of Biochar Application on Soil Properties, Plant Biomass Production, and Soil Greenhouse Gas Emissions: A Mini-Review. *Agric. Sci.* **2021**, *12*, 213–236. [CrossRef]

20. Yang, X.Y.; Chang, K.H.; Kim, Y.J.; Zhang, J.; Yoo, G. Effects of Different Biochar Amendments on Carbon Loss and Leachate Characterization from an Agricultural Soil. *Chemosphere* **2019**, *226*, 625–635. [CrossRef]

21. Ali, E.F.; Al-Yasi, H.M.; Kheir, A.M.S.; Eissa, M.A. Effect of Biochar on CO_2 Sequestration and Productivity of Pearl Millet Plants Grown in Saline Sodic Soils. *J. Soil Sci. Plant Nutr.* **2021**, *21*, 897–907. [CrossRef]

22. Zimmerman, A.R.; Gao, B.; Ahn, M.Y. Positive and Negative Carbon Mineralization Priming Effects among a Variety of Biochar-Amended Soils. *Soil Biol. Biochem.* **2011**, *43*, 1169–1179. [CrossRef]

23. Keiluweit, M.; Nico, P.S.; Johnson, M.; Kleber, M. Dynamic Molecular Structure of Plant Biomass-Derived Black Carbon (Biochar). *Environ. Sci. Technol.* **2010**, *44*, 1247–1253. [CrossRef] [PubMed]

24. Bruun, E.W.; Hauggaard-Nielsen, H.; Ibrahim, N.; Egsgaard, H.; Ambus, P.; Jensen, P.A.; Dam-Johansen, K. Influence of Fast Pyrolysis Temperature on Biochar Labile Fraction and Short-Term Carbon Loss in a Loamy Soil. *Biomass Bioenergy* **2011**, *35*, 1182–1189. [CrossRef]

25. Zhang, J.; Li, H.; Wang, Y.; Deng, J.; Wang, L. Multiple-Year Nitrous Oxide Emissions from a Greenhouse Vegetable Field in China: Effects of Nitrogen Management. *Sci. Total Environ.* **2018**, *616–617*, 1139–1148. [CrossRef]

26. Qi, Y.; Wu, Z.; Zhou, R.; Hou, X.; Yu, L.; Cao, Y.; Jiang, F. Nitrogen Reduction with Bio-Organic Fertilizer Altered Soil Microorganisms, Improved Yield and Quality of Non-Heading Chinese Cabbage (Brassica Campestris Ssp. Chinensis Makino). *Agronomy* **2022**, *12*, 1437. [CrossRef]

27. Wei, Q.; Xu, J.; Li, Y.; Liao, L.; Liu, B.; Jin, G.; Hameed, F. Reducing Surface Wetting Proportion of Soils Irrigated by Subsurface Drip Irrigation Can Mitigate Soil N_2O Emission. *Int. J. Environ. Res. Public Health* **2018**, *15*, 2747. [CrossRef]

28. Ning, D.; Qin, A.; Duan, A.; Xiao, J.; Zhang, J.; Liu, Z.; Liu, Z.; Zhao, B.; Liu, Z. Deficit Irrigation Combined with Reduced N-Fertilizer Rate Can Mitigate the High Nitrous Oxide Emissions from Chinese Drip-Fertigated Maize Field. *Glob. Ecol. Conserv.* **2019**, *20*, e00803. [CrossRef]

29. Wei, Q.; Li, X.; Xu, J.; Dai, H.; Li, B.; Xu, J.; Wei, Q.; Wang, K. Responses of Soil N_2O and CO_2 Emissions and Their Global Warming Potentials to Irrigation Water Salinity. *Atmosphere* **2022**, *13*, 1777. [CrossRef]

30. Searle, P.L. The Berthelot or Indophenol Reaction and Its Use in the Analytical Chemistry of Nitrogen. A Review. *Analyst* **1984**, *109*, 549–568. [CrossRef]

31. Hou, H.; Chen, H.; Cai, H.; Yang, F.; Li, D.; Wang, F. CO_2 and N_2O Emissions from Lou Soils of Greenhouse Tomato Fields under Aerated Irrigation. *Atmos. Environ.* **2016**, *132*, 69–76. [CrossRef]

32. Hamad, A.A.A.; Wei, Q.; Wan, L.; Xu, J.; Hamoud, Y.A.; Li, Y.; Shaghaleh, H. Subsurface Drip Irrigation with Emitters Placed at Suitable Depth Can Mitigate N_2O Emissions and Enhance Chinese Cabbage Yield under Greenhouse Cultivation. *Agronomy* **2022**, *12*, 745. [CrossRef]

33. Kuang, W.; Gao, X.; Gui, D.; Tenuta, M.; Flaten, D.N.; Yin, M.; Zeng, F. Effects of Fertilizer and Irrigation Management on Nitrous Oxide Emission from Cotton Fields in an Extremely Arid Region of Northwestern China. *F. Crop. Res.* **2018**, *229*, 17–26. [CrossRef]

34. Liu, G.; Li, Y.; Alva, A.K. High Water Regime Can Reduce Ammonia Volatilization from Soils under Potato Production. *Commun. Soil Sci. Plant Anal.* **2007**, *38*, 1203–1220. [CrossRef]

35. Weldon, S.; Rasse, D.P.; Budai, A.; Tomic, O.; Dörsch, P. The Effect of a Biochar Temperature Series on Denitrification: Which Biochar Properties Matter? *Soil Biol. Biochem.* **2019**, *135*, 173–183. [CrossRef]

36. Yang, W.; Feng, G.; Miles, D.; Gao, L.; Jia, Y.; Li, C.; Qu, Z. Impact of Biochar on Greenhouse Gas Emissions and Soil Carbon Sequestration in Corn Grown under Drip Irrigation with Mulching. *Sci. Total Environ.* **2020**, *729*, 138752. [CrossRef]

37. Karer, J.; Wimmer, B.; Zehetner, F.; Kloss, S.; Soja, G. Biochar Application to Temperate Soils: Effects on Nutrient Uptake and Crop Yield under Field Conditions. *Agric. Food Sci.* **2013**, *22*, 390–403. [CrossRef]

38. Rushimisha, I.E.; Li, X.; Han, T.; Chen, X.; Abdoul Magid, A.S.I.; Sun, Y.; Li, Y. Application of Biochar on Soil Bioelectrochemical Remediation: Behind Roles, Progress, and Potential. *Crit. Rev. Biotechnol.* **2022**, 1–9. [CrossRef]

39. Zhao, Y.; Li, X.; Li, Y.; Bao, H.; Xing, J.; Zhu, Y.; Nan, J.; Xu, G. Biochar Acts as an Emerging Soil Amendment and Its Potential Ecological Risks: A Review. *Energies* **2023**, *16*, 410. [CrossRef]

40. Hussain, R.; Ravi, K.; Garg, A. Influence of Biochar on the Soil Water Retention Characteristics (SWRC): Potential Application in Geotechnical Engineering Structures. *Soil Tillage Res.* **2020**, *204*, 104713. [CrossRef]

41. Sun, B.F.; Zhao, H.; Lü, Y.Z.; Lu, F.; Wang, X.K. The Effects of Nitrogen Fertilizer Application on Methane and Nitrous Oxide Emission/Uptake in Chinese Croplands. *J. Integr. Agric.* **2016**, *15*, 440–450. [CrossRef]

42. Ribas, A.; Mattana, S.; Llurba, R.; Debouk, H.; Sebastià, M.T.; Domene, X. Biochar Application and Summer Temperatures Reduce N_2O and Enhance CH_4 Emissions in a Mediterranean Agroecosystem: Role of Biologically-Induced Anoxic Microsites. *Sci. Total Environ.* **2019**, *685*, 1075–1086. [CrossRef] [PubMed]

43. Yang, F.; Lee, X.; Theng, B.K.G.; Wang, B.; Cheng, J.; Wang, Q. Effect of Biochar Addition on Short-Term N_2O and CO_2 Emissions during Repeated Drying and Wetting of an Anthropogenic Alluvial Soil. *Environ. Geochem. Health* **2017**, *39*, 635–647. [CrossRef] [PubMed]

44. Nair, V.D.; Nair, P.K.R.; Dari, B.; Freitas, A.M.; Chatterjee, N.; Pinheiro, F.M. Biochar in the Agroecosystem-Climate-Change-Sustainability Nexus. *Front. Plant Sci.* **2017**, *8*, 2051. [CrossRef]

45. Hua, L.; Lu, Z.; Ma, H.; Jin, S. Effect of Biochar on Carbon Dioxide Release, Organic Carbon Accumulation, and Aggregation of Soil. *Environ. Prog. Sustain. Energy* **2014**, *33*, 941–946. [CrossRef]

46. Kim, Y.S.; Makoto, K.; Takakai, F.; Shibata, H.; Satomura, T.; Takagi, K.; Hatano, R.; Koike, T. Greenhouse Gas Emissions after a Prescribed Fire in White Birch-Dwarf Bamboo Stands in Northern Japan, Focusing on the Role of Charcoal. *Eur. J. For. Res.* **2011**, *130*, 1031–1044. [CrossRef]

47. Yang, S.; Jiang, Z.; Sun, X.; Ding, J.; Xu, J. Effects of Biochar Amendment on CO_2 Emissions from Paddy Fields under Water-Saving Irrigation. *Int. J. Environ. Res. Public Health* **2018**, *15*, 2580. [CrossRef]

48. Lahijani, P.; Mohammadi, M.; Mohamed, A.R. Metal Incorporated Biochar as a Potential Adsorbent for High Capacity CO_2 Capture at Ambient Condition. *J. CO_2 Util.* **2018**, *26*, 281–293. [CrossRef]

49. Alburquerque, J.A.; Calero, J.M.; Barrón, V.; Torrent, J.; del Campillo, M.C.; Gallardo, A.; Villar, R. Effects of Biochars Produced from Different Feedstocks on Soil Properties and Sunflower Growth. *J. Plant Nutr. Soil Sci.* **2014**, *177*, 16–25. [CrossRef]

50. Ding, Y.; Liu, Y.; Liu, S.; Li, Z.; Tan, X.; Huang, X.; Zeng, G.; Zhou, L.; Zheng, B. Biochar to Improve Soil Fertility. A Review. *Agron. Sustain. Dev.* **2016**, *36*, 36. [CrossRef]

51. Biederman, L.A.; Stanley Harpole, W. Biochar and Its Effects on Plant Productivity and Nutrient Cycling: A Meta-Analysis. *GCB Bioenergy* **2013**, *5*, 202–214. [CrossRef]